Vanishing cyclotron gaps in a two-dimensional electron system with a strong short-period modulation

T. Feil,[1] K. Výborný,[2] L. Smrčka,[2] C. Gerl,[1] and W. Wegscheider[1]
[1]*Institut für Experimentalphysik, Universität Regensburg, 93040 Regensburg, Germany*
[2]*Institute of Physics, Academy of Sciences of the Czech Republic, Cukrovarnická 10, 16253 Praha, Czech Republic*
(Received 22 September 2006; published 1 February 2007)

Magnetotransport in a density-tunable two-dimensional electron gas that is modulated with a strong, atomically precise superlattice potential of a 15 nm period is investigated. For low densities, the system shows typical two-dimensional behavior. In the regime of large densities, however, a quasi-one-dimensional state is entered, in which the cyclotron gaps vanish and the quantum Hall effect breaks down. Both regimes, and the transition between them, are theoretically described in the framework of a quantum-mechanical tight-binding model.

DOI: 10.1103/PhysRevB.75.075303 PACS number(s): 73.23.−b, 73.43.Qt, 73.61.−r

The observation[1] and explanation[2] of the Weiss oscillations represent the first studies of a two-dimensional electron system (2DES) subject to a periodic modulation. Since then, many interesting new phenomena have been observed in such structures. Recent results include investigations of the Fermi surface[3,4] and of the Hofstadter butterfly.[5,6] However, all measurements reported on periodically modulated 2DES so far exhibit two-dimensional behavior in the form of the quantum Hall effect (QHE) at high magnetic fields. This can become different when a strong modulation potential is combined with a short periodicity.

All fabrication-dependent limitations on modulation period or strength were completely lifted with the introduction of the cleaved-edge overgrowth (CEO) process.[7] In this approach, the 2DES can be realized directly on the side of a superlattice (SL) structure, and it allows, therefore, an atomically precise modulation with almost arbitrary period and strength. A strong short-period modulation leads to the formation of minibands along the modulation direction which results for structures with wide minibands in a free two-dimensional magnetotransport behavior, albeit with a different effective mass.[8] Fundamental deviations from this behavior are predicted when the Fermi energy becomes larger than the miniband width.[9] So far, only once experiments in this extreme regime were presented.[9] In contrast to this study, we conclusively link the experimental data to the density of states (DOS) of the system and find good qualitative agreement in a direct comparison to theory without relying on fit parameters.

We investigate the magnetotransport in 2DESs with a strong short-period modulation in which the density or, equivalently, the Fermi energy of the system can be widely tuned. Even though the applied CEO method restricts us to a two-point measurement geometry, we show that it is possible to clearly separate the individual conductivity contributions to the measured resistance. This enables us to demonstrate that the system can enter both a two-dimensional and a one-dimensional transport regime according to the ratio between Fermi energy and miniband width. The typical free two-dimensional transport regime is found at relatively low densities. In contrast, a dominating Fermi energy results in a state in which the spin and cyclotron gaps have become unresolvably small. The system has become quasi-one-dimensional. The collapse of the two-dimensional behavior occurs for high densities and intermediate mobilities, which in conventional 2DESs are good conditions for the observation of the QHE. The transition from the two- to the one-dimensional state can be directly verified in the experimental data by a continuous shrinking of the cyclotron gaps.

The paper is organized in the following way. In Sec. I, the device structure is introduced. This is followed by a description of the observed density-dependent magnetoresistance oscillations in Sec. II. The theoretical model is detailed in Sec. III. Finally, in Sec. IV the experimental data are explained by the introduced quantum-mechanical tight-binding model, and a direct comparison of the experimental and theoretical magnetoresistance (MR) is presented.

I. DEVICE STRUCTURE

The samples investigated in this work are realized in two subsequent MBE growth steps (cf. the inset of Fig. 1). First, a 66-period $GaAs/Al_{0.3}Ga_{0.7}As$ SL is grown, sandwiched

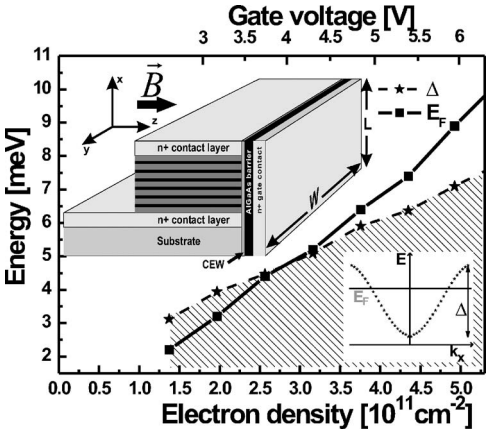

FIG. 1. Miniband width and Fermi energy of the 5 nm CEW sample plotted for increasing density. The voltage scale on the top axis connects the experimental gate voltage to the calculated densities and energy values. The inset shows a schematic drawing of the sample structure.

between two highly doped GaAs contact layers. The well and barrier widths are 12 and 3 nm, respectively. On both ends a well is placed right next to the contact layer. This structure is, then, *in situ* cleaved and overgrown with a GaAs well, referred to as the cleaved-edge well (CEW), followed by an $Al_{0.3}Ga_{0.7}As$ barrier and a highly doped GaAs gate contact. Structures with CEW widths of 1.6, 5, and 10 nm are investigated. The two doped layers next to the SL are used to contact the modulated 2DES that is established in the *x*-*y* plane by the application of a positive gate bias at the gate electrode. All structures have a width W to length L ratio of 500. Estimated mobilities of about 20 000, 25 000, and 30 000 cm^2/Vs are found for the 1.6, 5, and 10 nm CEW samples, respectively, from the onset of MR oscillations at a density of about 2.8×10^{11} cm^{-2}. Further details about the sample structure can be found in Refs. 10 and 11.

The ratio between the Fermi energy E_F and the miniband width Δ determines which state the electron system enters: two-dimensional at $E_F<\Delta$ or one-dimensional at $E_F>\Delta$. While the value of the applied gate voltage (V_G) controls the Fermi energy, the miniband width is determined by the SL properties, the CEW width, and V_G. Both a larger gate voltage and a wider CEW width shift the center of the electron wave functions further away from the SL potential. This reduces the modulation strength and results in wider minibands. The miniband width for different gate voltages can be calculated by a self-consistent solution of the Schrödinger and Poisson equations.[10] Figure 1 shows the density dependence of the miniband width for the 5 nm CEW sample. Even though the gate voltage leads to an increase of both the miniband width and the Fermi energy, a stronger dependence of the latter allows us to move the Fermi energy from inside the miniband at low densities (shaded region of Fig. 1) into the first minigap at larger densities (nonshaded region of Fig. 1). Experimentally, the transition from a two-dimensional to a one-dimensional state can be realized both for the 1.6 and 5 nm CEW samples. For the 10 nm CEW sample, the miniband width becomes so large that the densities necessary for the transition into the one-dimensional state can no longer be achieved. At the corresponding gate voltages, strong gate leakage currents develop that render the MR measurement meaningless.

II. DENSITY DEPENDENT MAGNETORESISTANCE

Figures 2(a) and 2(b) show typical MR data for a 5 nm CEW sample at small and large magnetic fields. The magnetic field is applied perpendicular to the two-dimensional electron system (cf. Fig. 1). The traces were measured with standard lock-in techniques at a temperature of 350 mK. The three gate voltages were chosen so that $E_F<\Delta$ at $V_G=3.5$ V, $E_F\gtrapprox\Delta$ at $V_G=5$ V, and $E_F>\Delta$ at $V_G=6.5$ V. In the low magnetic field regime, an increase of E_F leads to two prominent changes. A delayed onset of the MR oscillations is observed (marked by the gray triangles) and the position of the integer filling factors is shifted from maxima to minima. The latter observation can be extracted from Landau plots at small and large E_F. The delayed onset of the MR oscillations is only observed for $E_F>\Delta$ and does not occur in samples without modulation.

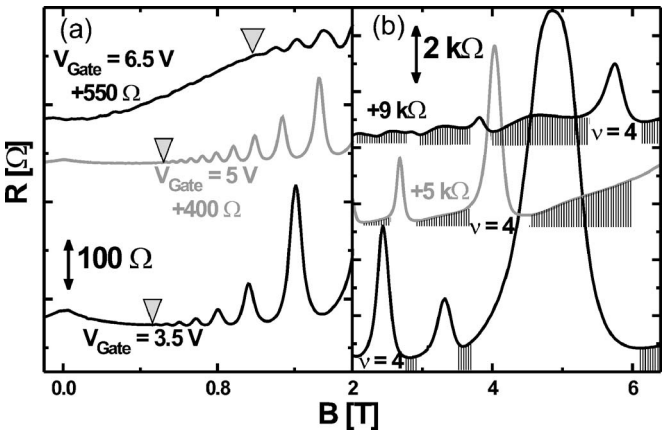

FIG. 2. (a) MR measurements for a 5 nm CEW sample at three different gate voltages in the small magnetic field regime. (b) Same traces at higher magnetic fields.

Changes in the MR at large magnetic fields due to an increasing Fermi energy are even more dramatic. At small E_F, large peaks appear that also mark the positions of integer filling. For the 10 nm CEW sample, such large peaks appear at all densities ($E_F<\Delta$ always) and the peak at $\nu=2$ eventually (above a certain magnetic field) reaches a plateau with the quantized resistance value $R=h/2e^2$ [cf. Fig. 5(a)]. This shows that the large MR peaks at small densities ($E_F<\Delta$) are indeed a signature of the QHE in these samples, confirming the two-dimensionality of the electron system in this regime. The large peaks of the 5 nm CEW sample at small E_F strongly shrink at large E_F and are replaced by a series of smaller features. At the same time, the shaded areas of Fig. 2(b), which denote regions of E_F between gaps in the DOS (noninteger ν) as we shall explain in Sec. III, strongly expand for increasing densities. The peak marked as $\nu=4$ eventually decreases in height with increasing E_F even though higher magnetic fields are necessary to reach $\nu=4$. The same is true for the peaks at filling factors 6 and 8. Peaks at higher filling factors completely vanish.

The MR data of the 1.6 nm CEW sample show similar behavior, however the closing of the cyclotron gaps starts already at a density of about 2.0×10^{11} cm^{-2} since the smaller CEW leads to a smaller miniband width[10] and, therefore, the condition $E_F>\Delta$ is reached at lower V_G.

III. THEORETICAL MODEL

The described behavior of the MR oscillations in Sec. II in dependence on E_F can be explained in terms of DOS calculations in a tight-binding approximation[9] (cf. Fig. 3). A comparison to experiment requires us to additionally find the relationship between the measured MR and the relevant quantities of the conductivity tensor σ. Since the sample geometry is wide and short, in contrast to the usual Hall bar, the electric field perpendicular to the modulation direction is negligibly small. This then leads to a measured resistance given by

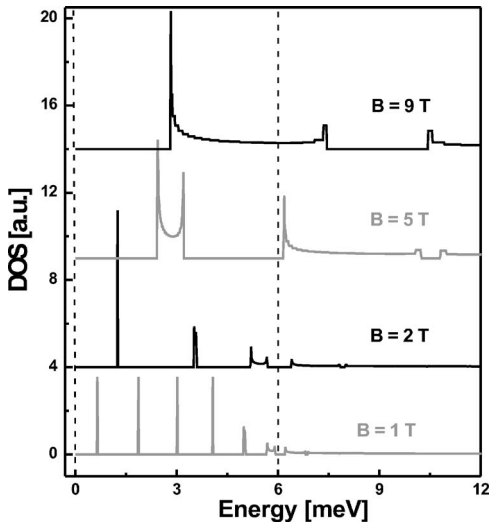

FIG. 3. DOS of a 2DES with strong short-period modulation calculated in tight-binding approximation for $\Delta=6$ meV. The dashed vertical lines mark the extension of the miniband.

$$R = \frac{U}{I} = \frac{F_x L}{j_x W + |j_y| L} = \frac{1}{\frac{W}{L}\sigma_{xx} + |\sigma_{xy}|}. \quad (1)$$

This equation has been shown to hold quantitatively by patterning Hall bar structures on modulation-doped CEO 2DES.[12] Thereby, it is assumed that the current density along both the x and y directions contributes to the total current. The electrons flowing along the y direction move toward the opposite electrode once they reach the boundaries of the sample. Even though Eq. (1) simultaneously contains contributions from the longitudinal and transversal conductivities, the geometry is nevertheless well suited to study the magnetotransport in the QHE regime. As long as $\sigma_{xx} \neq 0$, the large geometry factor W/L implies a relatively small R proportional to the scaled inverse of σ_{xx}. Only when the Fermi energy is in or very close to a cyclotron gap and σ_{xx} vanishes, the resistance is given by the larger (quantized) Hall resistance values. This is the correct limit for every two-point measurement on a sample with boundaries.[13] Equation (1) expresses the intuitive expectation for the given sample geometry. As long as there are extended states, they will directly connect the two electrodes and σ_{xx} determines the resistance. The Hall conductivity only contributes in the regime of localized states ($\sigma_{xx} \approx 0$). This intuitive understanding is clearly violated by the earlier experiments,[9] where the system becomes essentially insulating in the regime of extended states ($1/\sigma_{xx} \gtrsim 20$ MΩ between Hall plateaus). This results in fitting constants corresponding to unrealistically long relaxation times in Ref. 9. A possible origin of the experimental differences lies in a small structural difference at the edges of the sample.[14]

Combining Eq. (1) with the relation $\sigma_{xx} \sim$ DOS (following Ref. 9), we can beautifully explain the observed experimental data. The theoretical model is completely defined by two parameters, the period d and the hopping parameter $t=\Delta/4$ of the first miniband. The resulting eigenvalue problem is equivalent to that of a one-dimensional particle in the cosine potential $V(x)=2|t|[1-\cos(deBx/\hbar)]$,[9,15] which is generally known as the Mathieu-problem. When the Fermi energy is at the bottom of the cosine potential, i.e., the miniband width dominates, a quadratic expansion of the potential leads to equidistant Landau levels (LL) with a modified effective mass[8] as seen in Fig. 3 at small B ($R \propto 1/\sigma_{xx} \propto 1/\text{DOS}$). For such narrow LLs, the DOS is high and therefore the MR is small. Inside a DOS gap, the small overlap between the broadened LLs gives a large MR [$\sigma_{xx} \approx 0$ in Eq. (1)], which eventually approaches the quantized value $1/\sigma_{xy}$ [cf. Fig. 5(a), gray line]. This explains why integer filling factors correspond to resistance maxima at $E_F < \Delta$ in the experiment. When the Fermi energy, however, rises above the miniband, the cosine potential becomes a weak modulation for the one-dimensional particle and therefore wide bands separated by small gaps result, as can be seen in Fig. 3. In this limit, the LLs have broadened into wide bands with DOS singularities of $1/\sqrt{E}$ type at their edges (which can numerically not be fully resolved). When the broadened DOS singularities of neighboring bands overlap, the gap in between (where $\sigma_{xx} \approx 0$) is closed and the large σ_{xx} leads to a small MR at integer filling factor and thereby turns the maximum at small E_F into a minimum. This explains the experimentally observed switching from maxima to minima at integer ν. A similar observation was made for individual higher filling factors in 2DES with strong long-period modulation.[16] Also, DOS features at large E_F and small B are easily smeared by disorder so that the onset of MR oscillations are delayed up to larger magnetic fields in agreement with our findings in Fig. 2(a). For large magnetic fields, the gaps in the DOS are clearly visible at small and intermediate Fermi energies. However, at fixed B, an increasing E_F leads to successively smaller gaps. It can, therefore, be expected that disorder broadening closes all gaps above a certain filling factor. And this is, indeed, what is observed in the experiment. As Fig. 2(b) shows, at a small Fermi energy ($V_G=3.5$ V) the MR is dominated by wide DOS gaps, marked by peaks, with thin valleys (shaded) in between, which correspond to the inverse LLs of the DOS. These valleys broaden at larger E_F ($V_G=5$ V) into bands. However, their internal structure is only fully resolved when the Fermi energy becomes sufficiently large ($V_G=6.5$ V). The bands, then, inversely appear as additional broad peaks (maximum of $1/\sigma_{xx} \propto 1/\text{DOS}$ in the Landau band center) between those marking the shrinking DOS gaps. The fact that the DOS gaps are increasingly closed by disorder broadening is clearly documented in the experiment both by significantly smaller Hall resistance peaks at larger magnetic fields and by the absence of peaks for $\nu > 8$.

IV. DISCUSSION

The gradual collapse of the DOS gaps becomes even more evident when the MR data of the 5 nm CEW sample are plotted versus the inverse filling factor as shown in Fig. 4. With this rescaling, it is possible to directly follow the changes at individual filling factors when the gate voltage and thereby the Fermi energy is increased. Gaps at odd fill-

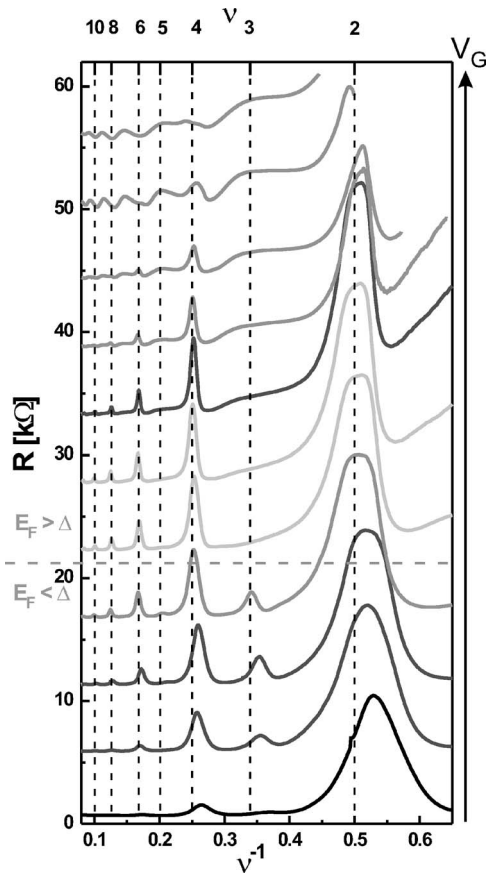

FIG. 4. MR data of the 5 nm CEW sample vs inverse filling factor. The gate voltage ranges from 2.5 to 7.5 V in 0.5 V steps. Higher gate voltage data are consecutively shifted upwards by 5.5 kΩ.

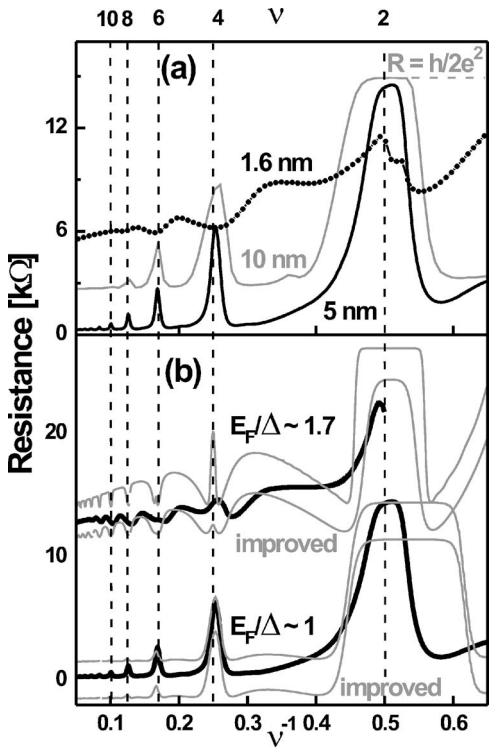

FIG. 5. (a) MR data of the 1.6 nm CEW (symbol, 5 kΩ shift), the 5 nm CEW (black line, no shift), and the 10 nm CEW (gray line, 2.5 kΩ shift) samples at a density of about 3.5×10^{11} cm^{-2}. (b) MR data of the 5 nm CEW sample (black lines) at gate voltages of 4.5 and 7 V (shifted upwards by 12 kΩ). The thin gray lines are theoretical calculations corresponding to the same densities. The theoretical lines are offset from the experimental data by +1.5 and −1.5 kΩ (marked "improved").

ing factors ($\nu=3$ and 5), which open up due to an enhancement of the g-factor, are only observed for $V_G\leq4$ V, which corresponds to the purely two-dimensional regime with $E_F<\Delta$. Once the Fermi energy exceeds the top of the miniband ($V_G\geq4.5$ V), the g-factor enhancement at $\nu=3,5$ appears to break down abruptly. In comparison, the closing of the DOS gaps at even filling factors occurs on a slower scale. The MR peaks marking $\nu=10$, 8, 6, and 4 vanish, respectively, when V_G exceeds 6, 6.5, 7, and 7.5 V. They are replaced by MR minima, which once again result from the overlap of DOS singularities of neighboring Landau bands. And even though the peak at $\nu=2$ survives at the highest manageable densities and magnetic fields, it is also substantially reduced. The vanishing of the DOS gaps at high densities leaves the system in a quasi-one-dimensional state. The possible quantization of the Hall resistance is lifted by the presence of extended states at the Fermi energy for all magnetic fields. Experimentally, this is observed in a transition of the MR from wide and large peaks (Hall plateaus) at small densities to that of smaller oscillations with opposite phase for $E_F\gg\Delta$.

By changing the miniband width, it is possible to either realize the one-dimensional state at lower densities or to avoid the collapse of the cyclotron gaps. This is illustrated by the MR data shown in Fig. 5(a). While for the 1.6 nm CEW and, therefore, smallest miniband width all cyclotron gaps have vanished (antiphase oscillations) and the DOS of a one-dimensional band structure is obtained, the 10 nm CEW data show a wide Hall plateau at $\nu=2$ with $R=h/2e^2$ and only broadened LLs (no bands) in between peaks (resistance minimum). The 5 nm CEW sample exhibits at $\nu=2$ no Hall plateau, but a peak larger than $R=h/2e^2$. This suggests that the enhancement of the g-factor, which has been neglected in our theory, cannot be ignored at these conditions. A strong influence from electron-electron interaction is also suggested by a strong temperature dependence of the same peak, not found for higher filling factors.

Finally, we compare the experimental data of the 5 nm CEW sample at $V_G=4.5$ and 7 V with MR calculations based on the tight-binding model combining σ_{xx} and σ_{xy} from Ref. 9 with Eq. (1). Disorder broadening is introduced in the form of an effective Dingle temperature $T_D=0.1$ meV, estimated from the observed onset of the MR oscillations. The imaginary part of the self-energy was chosen according to the transport relaxation time $\tau=0.8$ ps,[10,11] the Fermi energy and hopping parameter were taken from Fig. 1. The calculated MR [gray lines in Fig. 5(b)], which is independent of any fit parameters, confirms the experimentally observed features: an increasing Fermi energy leads to a vanishing of the cyclotron gaps (peaks at integer filling factors become smaller or vanish) while the signature of the internal Landau band

structure becomes visible (antiphase oscillations of the overlapping Landau bands). The agreement between theory and experiment improves somewhat when the Dingle temperatures and the transport relaxation times are individually adjusted for the two different densities using values close to the experimentally extracted ones. For the traces marked as improved in Fig. 5(b), the Dingle temperatures were chosen as T_D=0.1 and 0.3 meV, and the relaxation times as τ=1.6 and 1.1 ps at V_G=4.5 and 7 V, respectively. This shows that in order to achieve quantitative agreement, a more careful treatment of disorder including the dependence on density and magnetic field is necessary. Also, electron-electron interaction needs to be accounted for so that spin-related effects like the enhanced g-factor are properly described.

In conclusion, we have studied the MR of a 2DES subject to a strong short-period modulation. We show that, depending on the density, the 2DES can either enter a two-dimensional state with or a one-dimensional state without the presence of the DOS gaps. The MR of the 2D regime is marked by sharp maxima whenever the Fermi energy enters a DOS gap. In between these peaks, the broadened Landau levels lead to MR minima. In the 1D regime, the MR shows sharp minima at integer filling (E_F lies in a collapsed gap), and between these MR maxima due to the internal Landau band structure appear. The experimental data are in full agreement with the predictions of a quantum-mechanical tight-binding model. The realization of a one-dimensional state at $E_F > \Delta$ is characteristic for strong short-period modulations. The presented structures and the explanation of their MR provide an ideal basis for the study of 2DES with aperiodic one-dimensional modulation potentials.

ACKNOWLEDGMENTS

Financial support by the DFG via SFB348 and by the BMBF is gratefully acknowledged. K.V. and L.S. acknowledge the support of the Ministry of Education of the Czech Republic under Contract No. LC510 and the support of the Academy of Sciences of the Czech Republic through the Program No. KAN400100652.

[1] D. Weiss, K. v. Klitzing, K. Ploog, and G. Weimann, Europhys. Lett. **8**, 179 (1989).
[2] R. R. Gerhardts, D. Weiss, and K. v. Klitzing, Phys. Rev. Lett. **62**, 1173 (1989).
[3] C. Albrecht, J. H. Smet, D. Weiss, K. von Klitzing, R. Hennig, M. Langenbuch, M. Suhrke, U. Rössler, V. Umansky, and H. Schweizer, Phys. Rev. Lett. **83**, 2234 (1999).
[4] R. A. Deutschmann, W. Wegscheider, M. Rother, M. Bichler, G. Abstreiter, C. Albrecht, and J. H. Smet, Phys. Rev. Lett. **86**, 1857 (2001).
[5] C. Albrecht, J. H. Smet, K. von Klitzing, D. Weiss, V. Umansky, and H. Schweizer, Phys. Rev. Lett. **86**, 147 (2001).
[6] M. C. Geisler, J. H. Smet, V. Umansky, K. von Klitzing, B. Naundorf, R. Ketzmerick, and H. Schweizer, Phys. Rev. Lett. **92**, 256801 (2004).
[7] H. L. Stormer, L. N. Pfeiffer, K. W. Baldwin, K. W. West, and J. Spector, Appl. Phys. Lett. **58**, 726 (1991).
[8] A. Majumdar, L. Rokhinson, D. C. Tsui, L. N. Pfeiffer, and K. W. West, Appl. Phys. Lett. **76**, 3600 (2000).
[9] K. Výborný, L. Smrčka, and R. A. Deutschmann, Phys. Rev. B **66**, 205318 (2002).
[10] T. Feil, H.-P. Tranitz, M. Reinwald, and W. Wegscheider, Appl. Phys. Lett. **87**, 212112 (2005).
[11] T. Feil, C. Gerl, and W. Wegscheider, Phys. Rev. B **73**, 125301 (2006).
[12] M. Lermer, Ph.D. thesis, Universität Regensburg, http://www.opus-bayern.de/uni-regensburg/volltexte/2006/709/(2006).
[13] G. L. J. A. Rikken, J. A. M. M. van Haaren, W. van der Wel, A. P. van Gelder, H. van Kempen, P. Wyder, J. P. André, K. Ploog, and G. Weimann, Phys. Rev. B **37**, 6181 (1988).
[14] T. Feil, Ph.D. thesis, Universität Regensburg, http://www.opus-bayern.de/uni-regensburg/volltexte/2006/646/(2006).
[15] U. Wulf, J. Kučera, and A. H. MacDonald, Phys. Rev. B **47**, R1675 (1993).
[16] M. Tornow, D. Weiss, A. Manolescu, R. Menne, K. v. Klitzing, and G. Weimann, Phys. Rev. B **54**, 16397 (1996).